

Noise Suppression for Micromechanical Resonator via Intrinsic Dynamic Feedback

H. Ian,* Z. R. Gong, and C. P. Sun†

Institute of Theoretical Physics, The Chinese Academy of Sciences, Beijing, 100080, China

(Dated: October 27, 2018)

We study a dynamic mechanism to passively suppress the thermal noise of a micromechanical resonator through an intrinsic self-feedback that is genuinely non-Markovian. We use two coupled resonators, one as the target resonator and the other as an ancillary resonator, to illustrate the mechanism and its noise reduction effect. The intrinsic feedback is realized through the dynamics of coupling between the two resonators: the motions of the target resonator and the ancillary resonator mutually influence each other in a cyclic fashion. Specifically, the states that the target resonator has attained earlier will affect the state it attains later due to the presence of the ancillary resonator. We show that the feedback mechanism will bring forth the effect of noise suppression in the spectrum of displacement, but not in the spectrum of momentum.

PACS numbers: 85.85.+j, 85.25.Cp, 45.80.+r

I. INTRODUCTION

Recently, interests have been generated on cooling techniques for mechanical systems at nano- and micron-scales [1]. Among them, the typically employed is the feedback cooling technique where an external feedback circuit is responsible for detecting the motion of the target and feeding a counteracting force against this motion; through a general decrease of magnitude in the density noise spectrum, it was shown that the feedback can effectively reduce the fluctuation of the target and provide a cooling mechanism [3, 4]. Some experiments based on the models that contain the feedback loops have been carried out in the past few years. A few are directed towards the cooling of micron- to nanometer-size mechanical resonators, aiming to reach a macroscopic quantum mechanical ground state and serving as a powerful manifestation of quantum mechanical effects [5, 6, 7, 8]. Other experiments succeed in slowing down the motion of micron-size mirrors through the radiation pressure of an optical field in a Fabry-Pérot (FP) cavity, aiming to reach a noise level and equivalently an effective temperature that are pertinent to the employment of high-precision detection of gravity waves [9, 10, 11, 12].

The forementioned implementations of feedback cooling through reduction of noise fluctuations invariably rely on an electrical circuitry external to the target system to be cooled. The controller here is usually fixed and attracts or repels the resonator through either electrostatic Coulomb force or Lorentzian force. If such an external detection-control unit could be eliminated in favor of a mechanism with self-detection of and self-adjustment to the target's thermal motion, we call the mechanism "self-cooling" [13, 15]. Devices implementing this self-cooling use less components and are free from the reliance on an

external circuitry and hence prone to less noise sources.

In one case [13], an augmented cavity along with an extra optical cavity field is established on the other side of the mirror, in addition to the regular FP cavity, so as to counteract the radiation pressure from the original cavity field. This extra field cushions the motion of the pressure mirror and plays the role of feedback. In another case [14, 15], a set of Josephson junctions behaving as a qubit, serially connected to a mechanical resonating beam, serves delayed supercurrent into the circuit according to the magnetic flux through the circuit loop. The magnetic flux is controlled by the vibrating motion of the beam, which in turn is controlled by the magnetic field generated by the current feed. Such a mutual dependence furnishes a self-feedback mechanism. It should be pointed out that both of the self-feedback setups require delayed feedback, which assumed *a priori* a non-Markovian approximation that explicitly depends on the history of the target's motion. In these phenomenological treatments, the cooling target either couples itself to a static controller and makes itself prone to the noise stemmed from the feedback, or couples to a mechanically static detection construct and receives manually delayed feedback.

Hereby, we present a dynamic model based on an intrinsic mechanism with non-Markovian feedback, which is obviously free from an external feedback loop and does not rely on a presupposition of historical dependence. This mechanism is illustrated by a simple mechanical system in which the target is modeled by a harmonic oscillator and attached to a dynamic controller, which is a relatively heavier resonator, through a spring. The target is controlled by an intrinsic feedback through the dynamics of coupling: earlier positions and velocities of the target affects the motion of the controller and this influence is subsequently fed back to the target. Consequently, the accumulation of earlier states of the target will affect the state of itself later. With proper parameter setup, the target essentially experiences a resistance and decelerates its motion; its displacement variance is shrunk, noise suppressed and effective temperature cooled down. The lack

*Electronic address: hian@itp.ac.cn

†Electronic address: suncp@itp.ac.cn;

URL: <http://www.itp.ac.cn/suncp>

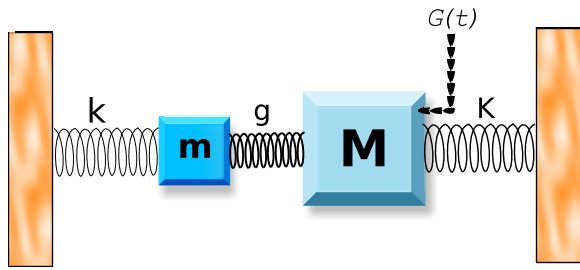


FIG. 1: (Color online) The diagrammatic figure shows the arrangement of the three springs and the two masses. From left to right, they are: the spring of constant k , the target mass m , the spring of constant g , the ancillary mass M , and the spring of constant K . $G(t)$ is the harmonic driving force.

of a specific detection device for the motion of the target resonator and an external feedback circuit characterizes the intrinsic nature of the mechanical feedback. Our numerical analysis shows the existence of a noise suppression capability of our scheme, e.g. the variance of displacement can be reduced to $0.04 \times 10^{-21} m^2$, and therefrom a cooling capability under a practical setting accessible in current experiments. We note that the scheme is theoretically illustrative through its simple model setup yet widely applicable because the general oscillator systems can be extended to quantum bosonic systems and other cases. In fact, a similar model and mechanism has been proposed to actively cool down the torsional vibration of a nanomechanical resonator through spin-orbit interactions [16].

The model will be explained in Sec.II and its delay function then derived *a posteriori* to examine its non-Markovian dependence. The complete solution of the system dynamics is given in Sec.III, with which we will derive the density noise spectrum and calculate the theoretical noise suppression rate. The associated numerical results will be presented in Sec.IV, given various parameter setups. The analysis is extended to the domain of momentum noise in Sec.V.

II. INTRINSIC FEEDBACK BY COUPLING DYNAMICS

A. The Model

Our model setup (see Fig.1) comprises two masses and three springs. The two masses are denoted by m and M , respectively. The mass m is the target and typically lighter whereas the mass M serves as an ancillary controller and is relatively heavier. The three springs are denoted by their Hooke's constants k , g and K , respectively. The spring of constant k attaches the lighter mass m to the fixed wall on the left and the spring of constant K attaches the heavier mass M to the fixed wall on the right. The spring of constant g strings the two masses together. Such a setup, intuitively, grants the heavier mass

M the function of a suspension system and a medium for the feedback. The symbol $G(t)$ represents an external driving force which is necessary for the discussion of cooling but can be deemed zero for the present.

The connected springs will give rise to mechanical vibrations of the masses. We let $\bar{\omega} = \sqrt{(k+g)/m}$ denote the effective mechanical resonance frequency for the mass m , assuming the other mass M is fixed, and $\bar{\Omega} = \sqrt{(K+g)/M}$ the equivalent for the mass M , assuming the mass m is fixed. Besides these mechanical vibrations, we assume each of the masses experience a frictional damping and we let γ denote the damping coefficient for the mass m and Γ that for mass M .

Then according to the setup above, the coordinates of the two masses obey a coupled system of classical Langevin equations

$$\ddot{x} + \gamma\dot{x} + \bar{\omega}^2 x - \frac{g}{m}Q = f \quad (1)$$

$$\ddot{Q} + \Gamma\dot{Q} + \bar{\Omega}^2 Q - \frac{g}{M}x = F \quad (2)$$

where x is the coordinate of the mass m and Q that of the mass M . f and F on the right hand side of the equations denote the random thermal noise generated by the mass m and M , respectively, due to their frictional damping.

The frictional damping terms as dissipation and the random noise terms as fluctuations constitute the total Brownian thermal force in the classical Langevin formalism. This thermal force induces an thermal environment, the effect of which is divided among the two terms $f(t)$ and $F(t)$ according to the fluctuation-dissipation relations [17]

$$\langle f(t)f(t') \rangle = 2k_B T \frac{\gamma}{m} \delta(t-t'), \quad (3)$$

$$\langle F(t)F(t') \rangle = 2k_B T \frac{\Gamma}{M} \delta(t-t'). \quad (4)$$

For now we assume the two masses are independently interacting with two thermal environments. That is, there are no correlations between the fluctuations of the two masses

Actually, we can realize from Eq.(1) and Eq.(3) that the motion of the mass m is resisted by a frictional force γ , which in turn is transduced into thermal energy and heats up itself. This process, however, is mediated by the mass M that stands between m and the fixed wall through the term $(g/M)Q$. If there were not the mass M , the kinetic oscillation of m would be instantly reacted by the surrounding springs of Hooke's constant k and K . With the presence of the mass M and the extra spring of constant g , the oscillation of the mass m will first squeeze the spring of constant g , and then the squeezed spring will release and push the mass M to the right. It follows that the spring of constant K will be squeezed successively. The mediating mass M breaks the original single spring into two and permits these two springs to stay in different states, squeezed and released, and hence essentially delays the reaction of the springs. This cascaded process is then reflected by the wall and executed

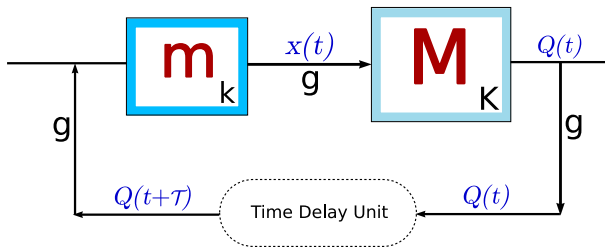


FIG. 2: Schematic illustration of the feedback mechanism shows the controller M receives signal $x(t)$ and outputs signal $Q(t)$ according to the motion of the target m .

in a reversed order to the left; the delayed reaction of the springs of constant g and K acts back onto the oscillating mass m . The delayed reaction depends on the oscillating velocity of the target mass m and can thus be considered a feedback onto itself.

The entire process can be regarded as a feedback loop from the view of control theory through the flow diagram shown in Fig.2. The target resonator m is the system to be controlled and the ancillary resonator M becomes the controller which detects the signal $x(t)$ as its input and feeds the signal $Q(t)$ as its output. The cycle time of the loop corresponds to the delay of the controller-to-system reaction. The dependence of this delayed reaction on the tunable parameters, mainly those spring constants, allows us to control this self-feedback precisely to counteract the oscillating motion of the target mass.

The weakened motion is converted to a reduction of effective temperature of the target mass through an equivalent relation between the autocorrelation of the target's displacement and temperature, derived from the fluctuation-dissipation relation Eq.(3). Under normal circumstances, that is, when the coupling mass M were not present, this equivalent relation can be written as

$$\langle x(t)x(t') \rangle = 2\pi k_B \gamma T \xi_0(t-t') \quad (5)$$

where γ is defined as in Eq.(1) and ξ_0 is a function to be given explicitly. Experimentally, the statistical variance of the coordinate is measured and the above relation is used to compute an effective temperature.

Increasing the damping coefficient γ will certainly increase the enveloping rate of the oscillating motion of $x(t)$. However, this reduction of motion cannot lead to an equivalent noise suppression effect upon the target mass m because of the constraint imposed by the friction-induced fluctuation relation described above. In fact, according to this relation, increasing damping rate leads to more thermal dissipation of the system. That is to say, simply enlarging frictional force merely results in a heating effect upon the target system. Our aim, therefore, is to reduce the temperature of the target mass by reducing its coordinate variance through the feedback that does not simultaneously increase the damping coefficient. After we derive the explicit feedback response below, we will show the feedback is actually shrinking the variance

in Sec.III.

B. The Feedback

Generally, a feedback external to an oscillating system has the effect of adding an extra driving force term on the right hand side of the equation of motion, i.e.

$$\ddot{y} + \gamma \dot{y} + \bar{\omega}^2 y = f + \mathcal{F}_{\text{fb}} \quad (6)$$

where we have let y denote the coordinate of a general dynamic system, \mathcal{F}_{fb} the feedback force, and $\gamma, \bar{\omega}, f$ terms of similar meanings to those defined in Eq.(1). If the target were to be cooled, the motion of the system should be slowed down. In other words, behaving as a function of the target's velocity, the force \mathcal{F}_{fb} should have an equivalent effect of increasing the damping coefficient, but do not increase the fluctuations. Besides, the feedback force should be dependent on the target's position and the noise source.

Summing up these requirements, we expect \mathcal{F}_{fb} to be a function of $y(t), \dot{y}(t)$ and f . To overcome the generic fluctuation-dissipation relations and hence accomplish an efficient noise suppression, we shall use a non-Markovian type feedback: \mathcal{F}_{fb} not only depends on the current value of the velocity and the position of the target, but also their historical values at past times. If we represent the historical dependence by a time-derivative $dK(y, \dot{y}, \tau)/d\tau$ and weigh the contribution of the histories by a delay function $h(t-\tau)$, where t stands for the current time and τ for the time in the past, the feedback force can be written as an integral with respect to τ ,

$$\mathcal{F}_{\text{fb}} = \int_{-\infty}^t d\tau \frac{dK(y, \dot{y}, \tau)}{d\tau} h(t-\tau). \quad (7)$$

The above formula shows the mathematical character of a general feedback force. Inversely, any function that can express the same character should be considered a feedback force. Therefore, we can verify the dynamic response of the coupling mass M in our model as an effective feedback mechanism by finding the corresponding specific expression for $K(y, \dot{y}, t)$ and $h(t-\tau)$. To do so, we solve Eq.(2) by using Fourier transforms and integration by parts (the detailed derivation is given in Appendix A)

$$Q(t) = \frac{1}{2\pi} \int_{-\infty}^{\infty} d\tau d\omega \frac{\frac{g}{M} x(\tau) + F(\tau)}{(\Omega^2 - \omega^2) + i\Gamma\omega} e^{-i\omega(\tau-t)} \quad (8)$$

$$= \frac{1}{\Omega^2} \phi(x, t) + \frac{2}{\sqrt{4\Omega^2 - \Gamma^2}} \times \int_{-\infty}^t d\tau \frac{d\phi(x, \tau)}{d\tau} h(t-\tau) \quad (9)$$

where

$$\phi(x, t) = \frac{g}{M} x(t) + F(t) \quad (10)$$

denotes the inhomogeneous part of the equation, i.e. the external driving force to M . In the solution,

$$h(\xi) = -\frac{1}{2\bar{\Omega}^2} \exp\left[-\frac{1}{2}\Gamma(\xi)\right] \left\{ \sqrt{4\bar{\Omega}^2 - \Gamma^2} \times \right. \quad (11)$$

$$\left. \cos\left[\frac{\xi}{2}\sqrt{4\bar{\Omega}^2 - \Gamma^2}\right] + \Gamma \sin\left[\frac{\xi}{2}\sqrt{4\bar{\Omega}^2 - \Gamma^2}\right] \right\}$$

is the delay function that we look for and

$$K(x, \tau) = \frac{2}{\sqrt{4\bar{\Omega}^2 - \Gamma^2}} \phi(x, \tau) \quad (12)$$

correspondingly shows the historical dependence.

If we plug the solution (9) into Eq.(1), i.e. reduce the degree of freedom of the variable $Q(t)$ in the equation by substituting with its formal solution, we arrive at an integro-differential equation of only a single variable $x(t)$, which is comparable to the feedback-containing equation of motion that appears in previous literature [12, 15]. However, in the latter case the delay function is assume to be a non-Markovian approximation

$$h(\xi) = 1 - e^{-r\xi} \quad (13)$$

and $K(y, \dot{y}, \tau)$ is left unknown. Here, we have explicitly implemented a self-feedback mechanism that exerts force back onto the mass m after certain delay through the use of the coupling mass M . The sinusoidal factor in the delay Eq.(11) illustrates the damped oscillating motion of the mass M . The implicit time derivative of $x(t)$ within the integrand implies up to an equivalent effect an additional friction to the motion of the mass m , which damps the oscillation without increasing the target's fluctuation. The non-integral term is Markovian and has the same order as $\bar{\omega}^2 x$. Though it does not appear in Eq.(7), this term effectively reduces the oscillating frequency and shall not counteract the feedback effect. Therefore, both terms impose noise suppression effect to our target. The only limitation, however, is the thermal fluctuation $F(t)$ from the coupling mass M itself and it will result in a limit for the suppression because of the competition between this fluctuation and the effective feedback.

III. EXACT SOLUTIONS OF THE LANGEVIN EQUATIONS

In order to examine the validity of the above proposed mechanism and verify the efficacy of the cooling rate, we find the analytic solutions of the Langevin equations (1) and (2) to reflect the displacement of the target m as a response to its own thermal noise, the motion of the ancillary mass M and the thermal noise of mass M . From the response function, we shall derive the effective damping coefficient and vibrating frequency of the target mass m as well as the autocorrelation function of its coordinate. The noise spectrum and the total noise fluctuation are then defined upon these derived quantities.

A. The Noise Spectrum

The displacement spectrum can be written as the sum of responses of the noise terms (the derivation is given in Appendix B)

$$\tilde{x}(\omega) = L_f(\omega)\tilde{f}(\omega) + L_F(\omega)\tilde{F}(\omega). \quad (14)$$

Note that the two different susceptibilities

$$L_f(\omega) = \frac{1}{\bar{\omega}_e^2 - \omega^2 + i\omega\gamma_e} \quad (15)$$

and

$$L_F(\omega) = \frac{g/m}{[\bar{\Omega}^2 - \omega^2 + i\omega\Gamma][\bar{\omega}_e^2 - \omega^2 + i\omega\gamma_e]} \quad (16)$$

reflect the system's different responses to thermal fluctuations from the mass m and the mass M . Here, we have defined the effective vibrating frequency of the mass m to be

$$\bar{\omega}_e^2(\omega) = \bar{\omega}^2 - \frac{g^2}{mM} \frac{\bar{\Omega}^2 - \omega^2}{(\bar{\Omega}^2 - \omega^2)^2 + \omega^2\Gamma^2} \quad (17)$$

and the effective damping coefficient of the mass m to be

$$\gamma_e(\omega) = \gamma + \frac{g^2}{mM} \frac{\Gamma}{(\bar{\Omega}^2 - \omega^2)^2 + \omega^2\Gamma^2}. \quad (18)$$

Eq.(14) means that the mechanical susceptibility or response function of the target m is adjusted because of the dynamic coupling of the target mass m to the ancillary mass M . The first term represents the direct effect of the thermal bath acting on the target mass m ; whereas the second term represents the indirect effect of the thermal bath onto the mass m through the mediating mass M and the coupling between the two masses.

The positivity of the second term in Eq.(18) has asserted our expectation of increasing the damping rate without increasing thermal force. We shall also note that an additional noise source $F(\omega)$ is imposed onto the adjusted susceptibility Eq.(15) due to the dynamic coupling. But seeing that it is divided by a frequency-squared term, we expect it to be negligible when the target mass m is not resonating at a frequency close to that of the mass M .

The density noise spectrum (DNS), which is defined by the equation

$$S_x(\omega) = \frac{1}{2\pi} \int_{-\infty}^{\infty} d\omega' \langle \tilde{x}(\omega)\tilde{x}(\omega') \rangle, \quad (19)$$

can thus be computed from Eq.(14)

$$S_x(\omega) = \frac{2k_B T}{m} \frac{\gamma_e}{(\bar{\omega}_e^2 - \omega^2)^2 + \omega^2\gamma_e^2}. \quad (20)$$

Comparing the above equation with the case when M is absent, i.e. when γ_e is degenerated to γ , we observe a general suppression at the noise peak and spreading of the noise spectrum.

B. Noise Suppression

The observable effect of the noise sources on the motion of the mass m is equivalent to the variance of the displacement of the mass m in time domain, which is defined as the average of the entire noise spectrum, i.e. the integral of the DNS of x ,

$$\langle x^2(t) \rangle = \frac{1}{2\pi} \int_{-\infty}^{\infty} d\omega S_x(\omega) \quad (21)$$

$$= \frac{k_B T}{m\pi} \int_{-\infty}^{\infty} \frac{\gamma_e}{(\bar{\omega}_e^2 - \omega^2)^2 + \omega^2 \gamma_e^2} d\omega. \quad (22)$$

The integral is computable after we approximate the effective damping rate and vibrating frequency by truncating their expansions shown in Appendix C. As a result, the variance is a variable of temperature and the spring constants

$$\langle x^2 \rangle|_{k,K,g} = k_B T \frac{g + K}{g(k + K) + kK}. \quad (23)$$

The noise fluctuation depends on the three spring constants k , K and g as its parameters, and is independent of the masses m and M and the damping rate γ and Γ of the resonators. We shall notice that the noise suppression effect for the target resonator is always present for all values the spring constant g takes. This ideal result is due to the non-Markovian feedback we derived in Sec.II, which always increases the effective damping while retaining the same fluctuations.

Eq.(23) shows a complex relation between itself and its three parameters of spring constants. To illustrate its behavior, we focus on its relation with the spring constant g . It is a monotonic decreasing function of g and its two limiting values are

$$\langle x^2 \rangle|_{g \rightarrow 0} = \frac{k_B T}{k} \quad (24)$$

$$\langle x^2 \rangle|_{g \rightarrow \infty} = \frac{k_B T}{k + K}, \quad (25)$$

which coincides with our expectation that enlarging the constant g will render the feedback more effective due to the enlarged feedback amplitude Eq.(10).

The symmetry between the target mass and the ancillary mass in the model setup allows us to compute the variance of the ancillary mass following the same methodology

$$\langle Q^2 \rangle|_{k,K,g} = k_B T \frac{g + k}{g(k + K) + kK}. \quad (26)$$

The limiting value of $\langle Q^2 \rangle$ at $g \rightarrow \infty$ is identical to that of $\langle x^2 \rangle$, which shows that under the extremal case where the two oscillating masses combines into one by a rigid body the limiting behaviors of the two bodies become the same.

IV. NUMERICAL ANALYSIS OF NOISE SUPPRESSION

To show completely the noise suppression behavior of the two oscillating masses, the numerical analysis is separated into two parts with each part for each extremal end of the values of the spring constants whereas the other parameters are set to laboratory accessible values for common micromechanical resonators. The first case, the identical case, is where the springs attaching the two masses to the walls share the same Hooke's constant, i.e. $k = K$. We examine how the noise suppression behavior is affected by varying the value of the constant g of the middle spring. The second case, the large detuning case, occurs when the springs attaching the two masses to the walls take vastly different values of their Hooke's constant. Again we examine the noise suppression limit for different values taken for the constant g of the middle spring.

A. The Identical Case

We assume the springs with one end fixed to walls have $k = K = 1Nm^{-1}$. The lighter target mass has $m = 1 \times 10^{-8}kg$ and its frictional damping rate $\gamma = 0.1s^{-1}$. The heavier ancillary mass has $M = 1 \times 10^{-6}kg$ and its frictional damping rate $\Gamma = 4s^{-1}$. When free from the stringing spring g , the target mass will oscillate at a natural frequency of $10kHz$ and the ancillary mass at $1kHz$. The system's initial temperature is set to room temperature $T = 295K$.

We first look at the density noise spectrum of the ancillary resonator when the middle spring is set to have its constant $g = 0.01Nm^{-1}$, $0.1Nm^{-1}$, $1Nm^{-1}$, $10Nm^{-1}$ and $100Nm^{-1}$ as shown in Fig.3. The noise peaks at the frequencies $\omega_c = 1005Hz$, $1044Hz$, $1223Hz$, $1376Hz$ and $1404Hz$.

We notice that when tuning the spring constant g , not only the peaking frequency is shifted to the right, the peak amplitude is reduced along with the increased value of g . This proves a general suppression in noise and an equivalent cooling effect to the system. The details of the spectrum and the spread width can be shown more apparently when we cluster the peaks together with a common frequency ω_c for their corresponding peaking frequencies, which is shown in Fig.4. The total noise fluctuation reached after suppression can be computed from the area under each curve in the figure, using Eq.(22). The attenuated noise levels corresponding to the 5 values of the spring g are, respectively, 4.03, 3.73, 2.72, 2.12 and 2.04 times a common factor of $10^{-21}m^2$.

The cooling effect for the target mass m is more obvious if we examine the clustered peak plot of the target mass' density noise spectrum shown in Fig.5. However, differing from the behavior of the ancillary mass shown in Fig.3, the target mass is resonant at two peak frequencies for each of the 5 values of the spring constant g . Among

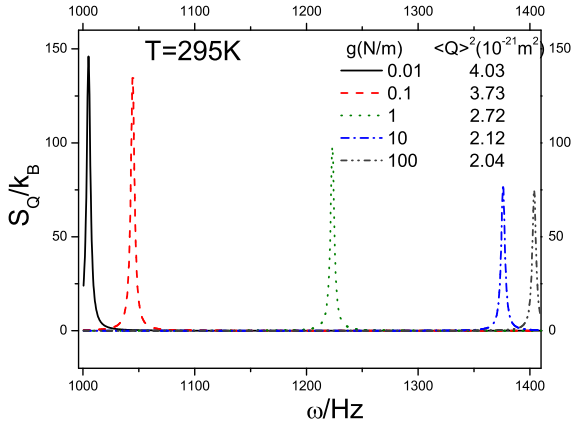


FIG. 3: (Color online) Plot of DNS of the ancillary resonator M with parameters: $k = K = 1Nm^{-1}$, $M = 1 \times 10^{-6}kg$, $m = 1 \times 10^{-8}kg$, $\Gamma = 4s^{-1}$, $\gamma = 0.1s^{-1}$, $T = 295K$. Curves from top to bottom are plotted from $g = 0.01Nm^{-1}$, $0.1Nm^{-1}$, $1Nm^{-1}$, $10Nm^{-1}$, $100Nm^{-1}$.

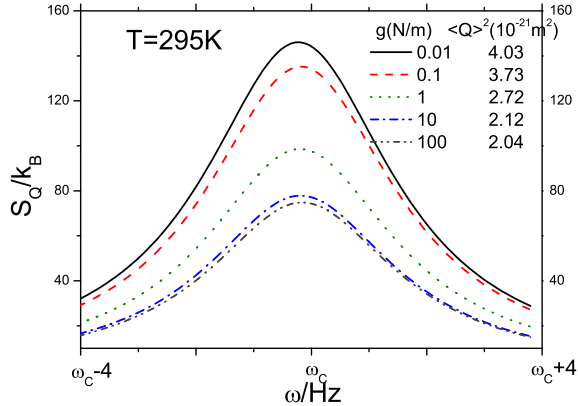


FIG. 4: (Color online) Rescaled plot of DNS of the ancillary resonator M with parameters: $k = K = 1Nm^{-1}$, $M = 1 \times 10^{-6}kg$, $m = 1 \times 10^{-8}kg$, $\Gamma = 4s^{-1}$, $\gamma = 0.1s^{-1}$, $T = 295K$ and peaking frequencies shifted to the center of the plot. Curves from top to bottom are plotted from $g = 0.01Nm^{-1}$, $0.1Nm^{-1}$, $1Nm^{-1}$, $10Nm^{-1}$, $100Nm^{-1}$.

the pairs of peaking frequencies, one group clusters in the low frequencies and the other spreads out in the high frequencies.

The low frequency group, the rescaled along peak center plot shown on the left of Fig.5, shares exactly the same peaking frequencies as those of the ancillary mass and we expect this behavior takes place when the target mass is resonating with the ancillary mass. This harmonic driven noise associates with the noise source $\tilde{F}(\omega)$ in Eq.(14) and, as we argue before, does not contribute much to the overall thermal noise. The high frequency group spreads out to peak frequencies $\omega_c = 10.1kHz$, $10.5kHz$, $14.2kHz$, $33.3kHz$ and $101kHz$ for the varying spring constant g . The anharmonic noise with respect to the ancillary mass associates with the noise source $\tilde{f}(\omega)$ in Eq.(14). Our cooling mechanism in this identical case

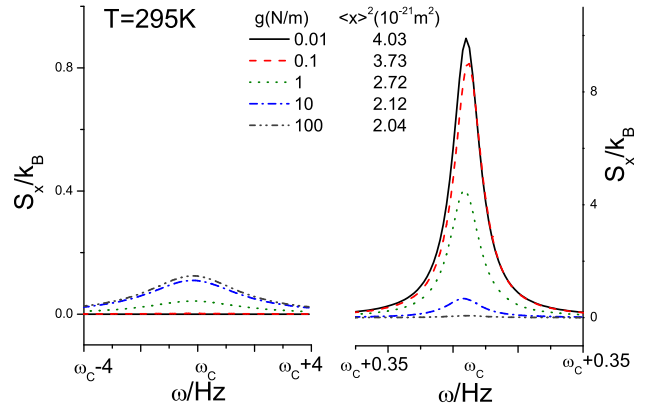


FIG. 5: (Color online) Rescaled plot of DNS of the target resonator m with parameters: $k = K = 1Nm^{-1}$, $M = 1 \times 10^{-6}kg$, $m = 1 \times 10^{-8}kg$, $\Gamma = 4s^{-1}$, $\gamma = 0.1s^{-1}$, $T = 295K$ and peaking frequencies shifted to the center of the plot. The left and the right subplots corresponds to the low and the high peak frequency groups. Curves from top to bottom are plotted from $g = 0.01Nm^{-1}$, $0.1Nm^{-1}$, $1Nm^{-1}$, $10Nm^{-1}$, $100Nm^{-1}$.

is fairly effective, with the noise level reached down to 4.03, 3.73, 2.72, 2.12 and 2.04 times a common factor of $10^{-21}m^2$, respectively, identical to the values of the ancillary mass.

B. The Large Detuning Case

We assume, in this case, the spring constants $K = 1000Nm^{-1}$ and $k = 1Nm^{-1}$; the masses $M = 1 \times 10^{-3}kg$ and $m = 1 \times 10^{-8}kg$; thus the natural oscillating frequencies for the two masses are retained. The damping coefficients and the initial temperature are left unchanged. Varying the spring constant of the middle spring g over the same five values gives the noise spectrum plot of the target mass m shown in Fig.6. The plot is again rescaled to the center along the peaking frequencies $\omega_c = 10.1kHz$, $10.5kHz$, $14.1kHz$, $33.2kHz$ and $100.5kHz$.

We note that the noise peaks at one frequency for each value of the spring g . These peaking frequencies are close to those in the identical case above but the noise suppression rate, as we have expected, is much better. That means the large detuning not only helps suppress the noise source stemmed from the coupling mass M to negligible amplitude but also makes the feedback more effective for countering the target's noise. The 5 values of the spring constant g corresponds to noise fluctuations of 4.03, 3.70, 2.03, 0.37 and 0.04 times a common factor of $10^{-21}m^2$.

Fig.7 shows the plot of the ancillary resonator's noise spectrum, again rescaled to the center along the peaking frequencies. These peaking frequencies are very close to those of the target mass. We predict that the large detuning between the springs K and k puts the ancillary mass M into a particularly passive role that reflects the

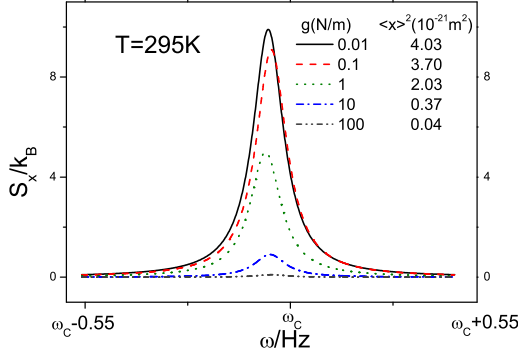


FIG. 6: (Color online) Rescaled plot of DNS of the target resonator m with parameters: $K = 1000Nm^{-1}$, $k = 1Nm^{-1}$, $M = 1 \times 10^{-3}kg$, $m = 1 \times 10^{-8}kg$, $\Gamma = 4s^{-1}$, $\gamma = 0.1s^{-1}$, $T = 295K$ and peaking frequencies shifted to the center of the plot. Curves from top to bottom are plotted from $g = 0.01Nm^{-1}$, $0.1Nm^{-1}$, $1Nm^{-1}$, $10Nm^{-1}$, $100Nm^{-1}$.

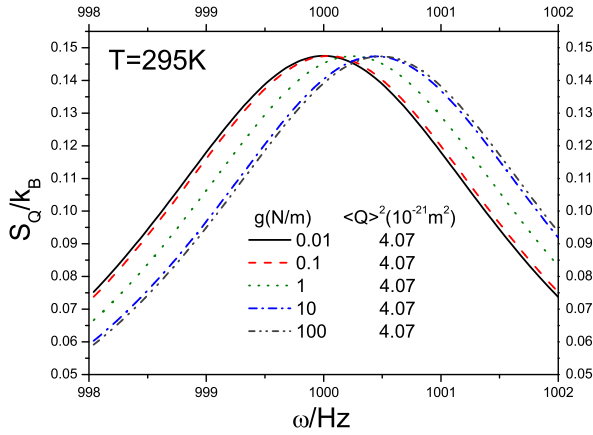


FIG. 7: (Color online) Rescaled plot of DNS of the ancillary resonator M with parameters: $K = 1000Nm^{-1}$, $k = 1Nm^{-1}$, $M = 1 \times 10^{-3}kg$, $m = 1 \times 10^{-8}kg$, $\Gamma = 4s^{-1}$, $\gamma = 0.1s^{-1}$, $T = 295K$ and peaking frequencies shifted to the center of the plot. Curves from left to right are plotted from $g = 0.01Nm^{-1}$, $0.1Nm^{-1}$, $1Nm^{-1}$, $10Nm^{-1}$, $100Nm^{-1}$.

minute motion of the target. This also helps explain why the noise suppression is especially effective in this case by the fact that the mass M has its speed comparable to the target m but in an opposite direction such that the force it exerts through the spring g can favorably counteract the motion of the target m . Nonetheless, the reinforced role that the ancillary mass M plays means that itself does not belong to the target system. As shown in the figure, the ancillary mass almost retains its original noise level throughout the varying values of the spring g .

V. NOISE IN MOMENTUM SPACE

A. The Model with Harmonic Driving Force

The effective temperature is usually defined according to the equipartition theorem through the equality between the thermal energy and the mechanical potential energy. The intrinsic nature of our model renders the stored potential energy of the target and of the environment in their shared link, the middle spring g , inseparable and thus forbids our discussion of the effective temperature in the coordinate space. To make our model relevant to the discussion of cooling, we examine the system dynamics in its momentum space and define the effective temperature according to the kinetic energy, i.e. the momentum fluctuation, of the target.

In addition, to follow the convention along previous literature, a harmonic driving force term

$$G(t) = F_0 e^{-i\omega_0 t}, \quad (27)$$

where ω_0 is the driving frequency, should be added to the feedback loop (Cf. Fig.1). In our case, this harmonic force appears as an extra term in the equation of motion of the ancillary resonator M .

Following the above arguments, we rewrite the coupled system of classical Langevin equations Eq.(1) and Eq.(2) as

$$\dot{p} + \gamma p + m\bar{\omega}^2 x - gQ = m f \quad (28)$$

$$\dot{P} + \Gamma P + M\bar{\Omega}^2 Q - gx = M(F + G(t)) \quad (29)$$

where $p = m\dot{x}$ and $P = M\dot{Q}$ denote, respectively, the momenta of the target resonator and the ancillary resonator. The thermal fluctuations f and F still obey the same set of relations Eq.(3) and Eq.(4).

Consequently, we have a modified linear response (Cf. Eq.(14), Eq.(15) and Eq.(16)) after combining the system of equations in the frequency domain (see Appendix D)

$$\begin{aligned} \tilde{p}(\omega) = i\omega m \left[L_f(\omega) \tilde{f}(\omega) + L_F(\omega) [\tilde{F}(\omega) \right. \\ \left. + 2\pi F_0 \delta(\omega + \omega_0)] \right] \end{aligned} \quad (30)$$

where $L_f(\omega)$ and $L_F(\omega)$ are the susceptibilities Eq.(15) and Eq.(16). We can thus arrive at the noise spectrum in momentum, after following the same routine of computations,

$$\begin{aligned} S_p(\omega) &= \frac{1}{2\pi} \int_{-\infty}^{\infty} d\omega' \langle \tilde{p}(\omega) \tilde{p}(\omega') \rangle \quad (31) \\ &= 2k_B T m \frac{\omega^2 \gamma_e}{(\bar{\omega}_e^2 - \omega^2)^2 + \omega^2 \gamma_e^2} + \\ &\quad 2\pi F_0^2 \omega_0^2 m^2 \delta(\omega + \omega_0) L_F(\omega_0) L_F(-\omega_0) \end{aligned} \quad (32)$$

B. The Effective Temperature

The square of momentum of the target is defined similarly as in Eq.(22)

$$\langle p^2 \rangle = \frac{1}{2\pi} \int_{-\infty}^{\infty} d\omega S_p(\omega). \quad (33)$$

which can be separated into two parts: the variance of momentum, i.e. the fluctuation or noise in momentum space,

$$\langle (\Delta p)^2 \rangle = \frac{k_B T}{\pi} m \int_{-\infty}^{\infty} d\omega \frac{\omega^2 \gamma_e}{(\bar{\omega}_e^2 - \omega^2)^2 + \omega^2 \gamma_e^2} \quad (34)$$

and the mean squared, i.e., the square of the steady state value of momentum,

$$\langle p \rangle^2 = F_0^2 \omega_0^2 m^2 L_F(\omega_0) L_F(-\omega_0). \quad (35)$$

Note that the harmonic force term only contributes to the first moment of the momentum.

Since thermal dissipation only induces variance of the target's momentum, the effective temperature of the target can inversely be determined by the variance of the kinetic energy through the energy equipartition theorem

$$T_{\text{eff}} = \frac{\langle (\Delta p)^2 \rangle}{2k_B m}. \quad (36)$$

Eq.(34) is independent of the two parameters F_0 and ω_0 of the harmonic driving force. We conclude that the harmonic force bears no effect in reducing the system's effective temperature and hence in cooling. Eq.(34) is also not analytically integrable, numerical integration shows the integral takes value similar to the case when the spring constant $g = 0$. That means the feedback is only effective in the displacement domain but not in the momentum domain.

VI. DISCUSSION AND REMARKS

In summary, we have proposed a theoretical model to demonstrate the general self-feedback type noise suppression technique through the coupling between the target resonator and an adjuvant system. In particular, such a self-feedback is achieved through the dynamics of the adjuvant system. The explicit delay function has been given and its efficacy in reducing the noise spectrum verified. We have also used numerical results to confirm our observations.

Before concluding this paper, we add some remarks as follows:

First, the theory of thermal equilibrium state can be used to explain why the system comprising two resonating masses has its noise reduced to a limit when the spring constant g tends from zero to infinity. If g were zero, the stringing spring between the two masses would

disappear and the system would comprise two independent resonators, each of which will attain its thermal equilibrium over time. In this case, the system has two degrees of freedom. According to the energy equipartition theorem, the system must contain twice as much energy as $k_B T/2$. For the other limit, when g tends to infinity, the two resonators become a rigid body and possess only one degree of freedom, which means the system would contain only $k_B T/2$ of energy. This explicit picture clarifies how the combined system reduces its energy over the increasing value of g .

However, how each resonator in the combined system reduces its own energy is an open question though we can intuitively think the heat bath may play crucial role in the asymmetric thermalization of the two resonators as a low open system. Another remark is that the energy equipartition theorem is applicable only after the system enters thermal equilibrium state. When interaction occurs between the two degrees of freedom contributed by the two masses, such an illustration is not appropriate. This is the reason why the nonlinear character of the noise suppression rate cannot be explained by the energy equipartition theorem alone.

In addition, we have assumed there does not exist correlation between the two noise sources for the two masses, i.e. $\langle f(t)F(t') \rangle = 0$. However, when the two masses oscillate very closely with each other, the above assumption based on independent thermal environments will not hold and we need to consider the case where

$$\langle f(t)F(t') \rangle \neq 0. \quad (37)$$

Another setting we shall consider is when the motions of the two masses are quantized: we need to change the fluctuation-dissipation relations Eq.(3) and Eq.(4) to

$$\langle f(t)f(t') \rangle \propto W(t, t', \hbar), \quad (38)$$

$$\langle F(t)F(t') \rangle \propto U(t, t', \hbar). \quad (39)$$

where W and U are not simply δ -functions and depends on the Planck constant \hbar . We will present the general investigation on the case with quantum fluctuations and thermal bath correlations, but here we have concentrated on the simple case.

Acknowledgments

The authors thank Yong Li of University of Basel and Ying Dan Wang of NTT Basic Research Laboratories for helpful discussions. This work is supported by the NSFC with Grants No.90203018, No.10474104, and No.60433050. It is also funded by the National Fundamental Research Program of China with Grants No.2001CB309310 and No.2005CB724508.

APPENDIX A: DERIVATION OF THE FEEDBACK DELAY FUNCTION

Fourier transforming Eq.(2) gives

$$\tilde{Q}(\omega) = \frac{g\tilde{x}(\omega)/M + \tilde{F}(\omega)}{\Omega^2 - \omega^2 + i\omega\Gamma} \quad (\text{A1})$$

where we use \tilde{x} , \tilde{Q} and \tilde{F} to denote the Fourier transforms of x , Q and F , respectively,

$$\tilde{x}(\omega) = \int_{-\infty}^{\infty} dt x(t)e^{-i\omega t}, \quad (\text{A2})$$

$$\tilde{Q}(\omega) = \int_{-\infty}^{\infty} dt Q(t)e^{-i\omega t}, \quad (\text{A3})$$

$$\tilde{F}(\omega) = \int_{-\infty}^{\infty} dt F(t)e^{-i\omega t}. \quad (\text{A4})$$

Substituting the first two transform of the above into Eq.(A1) and taking the inverse Fourier transform of \tilde{Q} , we get

$$Q(t) = \frac{1}{2\pi} \int_{-\infty}^{\infty} d\tau d\omega \frac{g x(\tau)/M + F(\tau)}{(\Omega^2 - \omega^2) + i\Gamma\omega} e^{-i\omega(t-\tau)}. \quad (\text{A5})$$

The linear integral with respect to ω can be viewed as a contour integral along a semicircle in the upper half-plane with two poles at $\omega_{\pm} = [i\Gamma \pm \sqrt{4\Omega^2 - \Gamma^2}]/2$. Assuming $\Gamma \ll \Omega$, the corresponding residues are,

$$R_{\pm}(t) = \mp \frac{1}{\sqrt{4\Omega^2 - \Gamma^2}} \theta(t - \tau) \times \exp \left[-\frac{1}{2} \left(\Gamma \mp i\sqrt{4\Omega^2 - \Gamma^2} \right) (t - \tau) \right] \quad (\text{A6})$$

where $\theta(t - \tau)$ denotes the unit step function originated from the positive locus of the integration path. Using Cauchy's theorem, $Q(t)$ is reduced to a single-integral form

$$Q(t) = \frac{2}{\sqrt{4\Omega^2 - \Gamma^2}} \int_{-\infty}^t d\tau \phi(x, \tau) \times \exp \left[-\frac{1}{2} \Gamma (t - \tau) \right] \sin \left[\frac{1}{2} \sqrt{4\Omega^2 - \Gamma^2} (t - \tau) \right] \quad (\text{A7})$$

where we have used the shorthand $\phi(x, t)$ as defined in Eq.(10). To write $Q(t)$ in our desired form, we further

integrate by parts with respect to $(t - \tau)$

$$\begin{aligned} Q(t) &= \frac{-2}{\sqrt{4\Omega^2 - \Gamma^2}} \int_0^{\infty} d(t - \tau) \phi(x, t) \quad (\text{A8}) \\ &\times \exp \left[-\frac{1}{2} \Gamma (t - \tau) \right] \sin \left[\frac{t - \tau}{2} \sqrt{4\Omega^2 - \Gamma^2} \right] \\ &= \frac{1}{\Omega^2} \phi(x, t) + \frac{2}{\sqrt{4\Omega^2 - \Gamma^2}} \times \quad (\text{A9}) \\ &\int_0^{\infty} d(t - \tau) \frac{d\phi(x, \tau)}{d(t - \tau)} 2 \exp \left[-\frac{1}{2} \Gamma (t - \tau) \right] \times \\ &\left\{ \frac{\exp \left[\frac{1}{2} i \sqrt{4\Omega^2 - \Gamma^2} (t - \tau) \right]}{\Gamma - i \sqrt{4\Omega^2 - \Gamma^2}} + \right. \\ &\left. \frac{\exp \left[-\frac{1}{2} i \sqrt{4\Omega^2 - \Gamma^2} (t - \tau) \right]}{\Gamma + i \sqrt{4\Omega^2 - \Gamma^2}} \right\} \end{aligned}$$

where the factor in the last two lines constitute the function $h(t - \tau)$ as defined in Eq.(11).

APPENDIX B: DERIVATION OF THE RESPONSE FUNCTION AND THE NOISE SPECTRUM

To find the response function, we first take the Fourier transform of Eq.(2) and Eq.(1) to get, respectively, Eq.(A1) and

$$\tilde{x}(\omega) = \frac{g\tilde{Q}(\omega)/m + \tilde{f}(\omega)}{\bar{\omega}^2 - \omega^2 + i\omega\gamma} \quad (\text{B1})$$

where we let \tilde{x} , \tilde{Q} and \tilde{f} denote the Fourier transforms of x , Q and f as we did in Appendix A. Substituting Eq.(A1) into Eq.(B1), we have

$$\tilde{x}(\omega) = \left(\frac{g}{m} \frac{g\tilde{x}(\omega)/M + \tilde{F}(\omega)}{\Omega^2 - \omega^2 + i\omega\Gamma} + \tilde{f}(\omega) \right) (\bar{\omega}^2 - \omega^2 + i\omega\gamma)^{-1} \quad (\text{B2})$$

Reshuffling the terms and putting again $\tilde{x}(\omega)$ on one hand side, the equation becomes

$$\tilde{x}(\omega) = \frac{\tilde{f}(\omega) + g\tilde{F}(\omega)/[m(\bar{\Omega}^2 - \omega^2 + i\omega\Gamma)]}{\bar{\omega}^2 - \omega^2 + i\omega\gamma - g^2/[mM(\bar{\Omega}^2 - \omega^2 + i\omega\Gamma)]}. \quad (\text{B3})$$

To find explicitly the response function, we group together the real terms and the imaginary terms in the denominator to write $\tilde{x}(\omega)$ in a familiar form similar to the case where the coupling mass M were not present; whence the denominator becomes

$$\begin{aligned} &\left[\bar{\omega}^2 - \frac{g^2}{mM} \frac{\bar{\Omega}^2 - \omega^2}{(\bar{\Omega}^2 - \omega^2)^2 + \omega^2\Gamma^2} \right] - \omega^2 \\ &+ i\omega \left[\gamma + \frac{g^2}{mM} \frac{\Gamma}{(\bar{\Omega}^2 - \omega^2)^2 + \omega^2\Gamma^2} \right] \quad (\text{B4}) \end{aligned}$$

and we can define the terms in the two brackets as in Eq.(17) and Eq.(18).

Using Eq.(14), the associated fluctuation-dissipation relations of Eq.(3) and Eq.(4) in the frequency domain

$$\langle \tilde{f}(\omega)\tilde{f}(\omega') \rangle = 4\pi k_B T \frac{\gamma}{m} \delta(\omega + \omega'), \quad (\text{B5})$$

$$\langle \tilde{F}(\omega)\tilde{F}(\omega') \rangle = 4\pi k_B T \frac{\Gamma}{M} \delta(\omega + \omega'), \quad (\text{B6})$$

and the independence between the two noise sources, we find by using definition Eq.(19)

$$S_x(\omega) = 2k_B T \left[\frac{\gamma}{m} L_f(\omega)L_f(-\omega) + \frac{\Gamma}{M} L_F(\omega)L_F(-\omega) \right] \quad (\text{B7})$$

where $L_f(\omega)$ and $L_F(\omega)$ are defined in Eq.(15) and Eq.(16). Seeing that

$$L_F(\omega) = \frac{g/m}{\Omega^2 - \omega^2 + i\omega\Gamma} L_f(\omega), \quad (\text{B8})$$

we can factor out $L_f(\omega)L_f(-\omega)/m$ from the bracket in Eq.(B7)

$$S_x(\omega) = \frac{2k_B T}{m} L_f(\omega)L_f(-\omega) \times \quad (\text{B9})$$

$$\begin{aligned} & \left[\gamma + \frac{g^2\Gamma/mM}{\Omega^2 - \omega^2 + i\omega\Gamma} \frac{1}{\Omega^2 - \omega^2 - i\omega\Gamma} \right] \\ &= \frac{2k_B T}{m} \left[\frac{1}{(\bar{\omega}_e^2 - \omega^2)^2 + \omega^2\gamma_e^2} \right] \times \quad (\text{B10}) \\ & \left[\gamma + \frac{g^2}{mM} \frac{\Gamma}{(\Omega^2 - \omega^2)^2 + \omega^2\Gamma^2} \right] \end{aligned}$$

which equals to Eq.(20).

APPENDIX C: DERIVATION OF THE VARIANCE OF DISPLACEMENT

The integrand of Eq.(22) has highest order of ω^4 in the denominator and can not be integrated analytically. To make the integrand integrable, we introduce a parameter $\mu(K) = g/(g+K)$ as a variable of the spring constant K and approximate the integrand by expanding $\bar{\omega}_e^2$ with respect to μ up to 2nd order in the vicinity of $\mu = 0$, in other words, when $K \rightarrow \infty$. That is, we let

$$\bar{\omega}_e^2(\mu) \approx \bar{\omega}_e^2|_{\mu=0} + \frac{d\bar{\omega}_e^2}{d\mu} \Big|_{\mu=0} \mu + \frac{1}{2} \frac{d^2\bar{\omega}_e^2}{d\mu^2} \Big|_{\mu=0} \mu^2. \quad (\text{C1})$$

To calculate the three terms in the expansion, we first substitute K with $g(1-\mu)/\mu$ in Eq.(17),

$$\bar{\omega}_e^2(\mu) = \bar{\omega}^2 - \frac{g^2}{mM} \frac{gM^{-1}\mu^{-1} - \omega^2}{(gM^{-1}\mu^{-1} - \omega^2)^2 + \omega^2\Gamma^2}. \quad (\text{C2})$$

Since the lowest-order term in the numerator and the denominator is, respectively, μ^{-1} and μ^{-2} , the second

term of the above formula goes to 0 when $\mu \rightarrow 0$. Thus we find the first term in the expansion $\bar{\omega}_e^2|_{\mu=0} = \bar{\omega}^2$. The first-order derivative of $\bar{\omega}_e^2(\mu)$ reads

$$\frac{d\bar{\omega}_e^2}{d\mu} = \frac{g^3}{mM^2} \frac{\mu^{-2} [-(gM^{-1}\mu^{-1} - \omega^2)^2 + \omega^2\Gamma^2]}{[(gM^{-1}\mu^{-1} - \omega^2)^2 + \omega^2\Gamma^2]^2}. \quad (\text{C3})$$

Again by comparing the coefficients of the lowest-order terms in the numerator and the denominator, we shall see the second term in the expansion $d\bar{\omega}_e^2/d\mu|_{\mu=0} = -g/m$. The third term in the expansion can be obtained similarly by observing the limiting behavior of the numerator and the denominator of the second-order derivative of $\bar{\omega}_e^2(\mu)$

$$\frac{d^2\bar{\omega}_e^2}{d\mu^2} \Big|_{\mu=0} = \lim_{\mu \rightarrow 0} \frac{g^3}{mM^2} \frac{-2gM^{-1}\mu^{-4}(gM^{-1}\mu^{-1} - \omega^2)^2}{[(gM^{-1}\mu^{-1} - \omega^2)^2 + \omega^2\Gamma^2]^3}, \quad (\text{C4})$$

which reads $-2(M/m)\omega^2$ after taking the limit. Combining the results, we have

$$\bar{\omega}_e^2 \approx \bar{\omega}^2 - \frac{g}{m}\mu - \frac{M}{m}\omega^2\mu^2. \quad (\text{C5})$$

The truncation error rate introduced in this approximation, by comparing Eq.(C2) and Eq.(C5), is

$$\text{erf} = \frac{\Delta\bar{\omega}_e^2}{\bar{\omega}_e^2} = \frac{\bar{\omega}_e^2 - [\bar{\omega}^2 - (g\mu - M\omega^2\mu^2)/m]}{\bar{\omega}_e^2}. \quad (\text{C6})$$

Expanding $\bar{\omega}_e^2$ and μ gives

$$\begin{aligned} \text{erf} &= \left\{ \left[\frac{g^2}{g+K} + \frac{M\omega^2g^2}{(g+K)^2} \right] (F^2 + M^2\omega^2\Gamma^2) - g^2F \right\} \\ &\times [(g+k)(F^2 + M^2\omega^2\Gamma^2) - g^2F]^{-1} \quad (\text{C7}) \end{aligned}$$

where we have used the shorthand $F = g + K - M\omega^2$. Since we only consider the usual cases with $\Gamma \ll \omega$, the terms containing the damping coefficient can be omitted

$$\text{erf} = \frac{[g^2/(g+K) + M\omega^2g^2/(g+K)^2]F - g^2}{(g+k)F - g^2}. \quad (\text{C8})$$

Expanding F and multiplying the numerator and denominator by $(g+K)^2$, we find

$$\left| \frac{\Delta\bar{\omega}_e^2}{\bar{\omega}_e^2} \right| = \frac{g^2M^2\omega^4}{(g+K)^2 [g(k+K - M\omega^2) + k(K - M\omega^2)]} \quad (\text{C9})$$

and at the other extreme of the expansion $\mu = 1$ whence $K = 0$ and g can take any value

$$\text{erf}|_{K=0} = \frac{M^2\omega^4}{g(k - M\omega^2) - kM\omega^2}. \quad (\text{C10})$$

Therefore, the error can be sufficiently suppressed if we let $g \rightarrow \infty$ and the expansion of $\bar{\omega}_e^2$ around $\mu = 1$ is validated.

Following the same reasoning and procedure, we can approximate the effective damping coefficient Eq.(18),

$$\gamma_e \approx \gamma + \frac{M\Gamma}{m}\mu^2 \quad (\text{C11})$$

which becomes ω -independent. Substituting Eq.(C5) and Eq.(C11) into Eq.(22), we get, after minor algebra,

$$\langle x^2(t) \rangle = \frac{k_B T \gamma'^2}{m \pi \gamma_e} \int_{-\infty}^{\infty} \frac{1}{(\bar{\omega}'^2 - \omega^2)^2 + \omega^2 \gamma'^2} d\omega \quad (\text{C12})$$

where

$$\gamma' = \frac{\gamma + (M\Gamma/m)\mu^2}{(M/m)\mu^2 + 1} \quad (\text{C13})$$

$$\bar{\omega}' = \sqrt{\frac{\bar{\omega}^2 - (g/m)\mu}{(M/m)\mu^2 + 1}} \quad (\text{C14})$$

can be considered the effective damping coefficient and vibrating frequency of the mass m after the approximation. We can apply a limiting process to Eq.(C12)

$$\langle x^2(t) \rangle = \frac{k_B T \gamma'^2}{m \pi \gamma_e} \lim_{t \rightarrow 0} \int_{-\infty}^{\infty} \frac{e^{-i\omega t}}{(\bar{\omega}'^2 - \omega^2)^2 + \omega^2 \gamma'^2} d\omega \quad (\text{C15})$$

and compute the integral using the theorem of residues as we did in Appendix A

$$\langle x^2(t) \rangle = \frac{k_B T \gamma'}{m \gamma_e \bar{\omega}'^2} \quad (\text{C16})$$

$$= k_B T \frac{g + K}{g(k + K) + kK}. \quad (\text{C17})$$

APPENDIX D: DERIVATION OF EFFECTIVE TEMPERATURE

Fourier transforming the Langevin equations in the momentum space Eq.(28) and Eq.(29) and recognizing

$$\tilde{p}(\omega) = i\omega \tilde{x}(\omega) \quad (\text{D1})$$

$$\tilde{P}(\omega) = i\omega \tilde{Q}(\omega), \quad (\text{D2})$$

we have

$$(\bar{\omega}^2 - \omega^2 + i\omega\gamma)\tilde{p}(\omega) - \frac{g}{M}\tilde{P}(\omega) = i\omega m\tilde{f}(\omega) \quad (\text{D3})$$

$$(\bar{\Omega}^2 - \omega^2 + i\omega\Gamma)\tilde{P}(\omega) - \frac{g}{m}\tilde{p}(\omega) = i\omega M(\tilde{F}(\omega) + 2\pi F_0\delta(\omega + \omega_0)). \quad (\text{D4})$$

We can follow the lines in Appendix B at this point to get the Fourier transform of the momentum of the target resonator

$$\tilde{p}(\omega) = i\omega \left[m\tilde{f}(\omega) + g \frac{\tilde{F}(\omega) + 2\pi F_0\delta(\omega + \omega_0)}{\bar{\Omega} - \omega^2 + i\omega\Gamma} \right] \times \left[\bar{\omega}^2 - \omega^2 + i\omega\gamma - \frac{g}{mM} \frac{1}{\bar{\Omega} - \omega^2 + i\omega\Gamma} \right]^{-1} \quad (\text{D5})$$

which can be written in a compact form as in Eq.(30) after grouping the terms. The density noise spectrum in momentum can then be computed

$$S_p(\omega) = \frac{1}{2\pi} \int_{-\infty}^{\infty} d\omega' \langle \tilde{p}(\omega)\tilde{p}(\omega') \rangle \quad (\text{D6})$$

$$= 2k_B T \omega^2 m^2 \left[\frac{\gamma}{m} L_f(\omega)L_f(-\omega) + \frac{\Gamma}{M} L_F(\omega)L_F(-\omega) \right] \quad (\text{D7})$$

$$+ 2\pi F_0^2 \omega^2 m^2 \delta(\omega + \omega_0) L_F(\omega)L_F(-\omega_0) \\ = 2k_B T m \frac{\omega^2 \gamma_e}{(\bar{\omega}_e^2 - \omega^2)^2 + \omega^2 \gamma_e^2} + \quad (\text{D8}) \\ + 2\pi F_0^2 \omega_0^2 m^2 \delta(\omega + \omega_0) L_F(\omega_0)L_F(-\omega_0)$$

-
- [1] K. Karrai, *Nature* **444**, 41 (2006).
[2] S. Mancini, D. Vitali, and P. Tombesi, *Phys. Rev. Lett.* **80**, 688 (1998).
[3] A. Hopkins, K. Jacobs, S. Habib, and K. Schwab, *Phys. Rev. B* **68**, 235328 (2003).
[4] B. D'Urso, B. Odom, and G. Gabrielse, *Phys. Rev. Lett.* **90**, 043001 (2003).
[5] P. F. Cohadon, A. Heidmann, and M. Pinard, *Phys. Rev. Lett.* **83**, 3174 (1999).
[6] A. Naik, O. Buu, M. D. LaHaye, A. D. Armour, A. A. Clerk, M. P. Blencowe, and K. C. Schwab, *Nature* **443**, 193 (2006).
[7] M. D. LaHaye, O. Buu, B. Camarota, and K. C. Schwab, *Science* **304**, 74 (2004).
[8] P. Zhang, Y. D. Wang, C. P. Sun, *Phys. Rev. Lett.* **95**, 097204 (2005).
[9] C. H. Metzger and K. Karrai, *Nature* **432**, 1002 (2004).
[10] O. Arcizet, P. Cohadon, T. Briant, M. Pinard, and A. Heidmann, *Nature* **444**, 71 (2006).
[11] S. Gigan, H. R. Boehm, M. Paternostro, F. Blaser, G. Langer, J. B. Hertzberg, K. C. Schwab, D. Baeuerle, M. Aspelmeyer, and A. Zeilinger, *Nature* **444**, 67 (2006).
[12] D. Kleckner and D. Bouwmeester, *Nature* **444**, 75 (2006).
[13] M. Bhattacharya and P. Meystre, *quant-ph/0704.2425*.
[14] F. Xue, Y. D. Wang, C. P. Sun, H. Okamoto, H. Yamaguchi, and K. Semba, *New J. Phys.* **9**, 35 (2007).
[15] Y. D. Wang, K. Semba and H. Yamaguchi, *cond-mat/0704.2462*; Fei Xue, Y. D. Wang, Yu-xi Liu, Franco Nori, *quant-ph/0706.3100*
[16] N. Zhao, D. L. Zhou, J. L. Zhu, C. P. Sun, *cond-mat.mes-hall/0705.1964*.
[17] R. Kubo M. Toda and N. Hashitsume, *Statistical Physics II* (Springer, 1985).